Repository Istituzionale dei Prodotti della Ricerca del Politecnico di Bari

Dosimetric characterization and image quality assessment in Breast Tomosynthesis

This is a post print of the following article

Original Citation:
Dosimetric characterization and image quality assessment in Breast Tomosynthesis / Andria, Gregorio; Attivissimo, Filippo; DI NISIO, Attilio; Lanzolla, Anna Maria Lucia; Maiorana, A; Mangiantini, M; Spadavecchia, Maurizio. - In: IEEE TRANSACTIONS ON INSTRUMENTATION AND MEASUREMENT. - ISSN 0018-9456. - STAMPA. - 66:10(2017), pp. 2535-2544. [10.1109/TIM.2017.2692318]

Availability:
This version is available at http://hdl.handle.net/11589/103287 since: 2021-03-09

Published version
DOI:10.1109/TIM.2017.2692318

Publisher:

Terms of use:

(Article begins on next page)

07 May 2024

Published Source
G. Andria, F. Attivissimo, A. Di Nisio, A.M.L. Lanzolla, A. Maiorana, M. Mangiantini and M. Spadavecchia, "Dosimetric Characterization and Image Quality Assessment in Breast Tomosynthesis", IEEE Transactions on Instrumentation and Measurement, vol. 66, no. 10, pp. 2535 - 2544 October 2017, doi: 0.1109/TIM.2017.2692318

Dosimetric Characterization and Image Quality Assessment in Breast Tomosynthesis

Gregorio Andria, *Member, IEEE*, Filippo Attivissimo, *Member, IEEE*, Attilio Di Nisio, *Member, IEEE*, Anna M. L. Lanzolla, *Member, IEEE*, Alberto Maiorana, Marco Mangiatini, and Maurizio Spadavecchia, *Member, IEEE*

***Abstract*— The aim of this paper was to investigate the diagnostic potential of tomosynthesis imaging compared with the performance of 2-D digital mammography in terms of radiation dose and image quality. In particular, suitable dosimeter and phantom were used for quantifying the average glandular dose and image quality parameters, respectively. First, according to standard protocols and European guidelines, the characterization of the used tomosynthesis system was carried out to verify the reliability of characteristic parameters of the system. Successively, the absorbed dose was calculated by means of experimental measurements and the application of estimation methods. The calculated dose was then compared with the value provided by the system; this approach has confirmed the tendency of mammography equipment manufacturers to underestimate the mean glandular dose. Finally, the detection capability of different details with different contrasts was objectively assessed for both breast tomosynthesis and 2-D mammography.**

***Index Terms*— Digital radiography, image quality, radiation dose, tomosynthesis.**

I. Introduction

BREAST cancer is the most common cancer in women. Recent decades, the diffusion and improvement of screening procedures have led to an increase in the early breast cancer diagnosis and a consequent reduction in mortality of more than 20% [1], [2]. Medical imaging techniques, such as computed tomography (CT), magnetic resonance imaging (MRI), ultrasound and digital radiography, generally offer a low contrast between tissues under examination and background features, thus reducing the ability to detect and characterize lesions or abnormalities. Therefore, the development of suitable techniques to improve sensitivity and image quality plays a very important role in diagnostic medical imaging [3]–[6].

Breast ultrasound imaging is easy to use and provides real-time images. It is commonly used as an adjunct to diagnostic clinical mammography because it can cause unacceptable false positive and false negative outcomes, especially in asymptomatic women [7]. MRI breast cancer screening instead is recommended for women with a higher risk of breast cancer. It has good image resolution and is effective for evaluating dense breasts. Its main limitations are that is time consuming, more expensive, and may not show all calcifications [8].

Systems based on time-domain reflectometry or spectroscopy, with microwave or near-infrared electromagnetic radiation, can detect the different liquid content of malignant tissues [9]–[12]. They have the advantage of being safer with respect to the use of ionizing radiation; however, their resolution is lower than X-ray mammography and is still under development.

The main limit of conventional mammography is the superposition of signals from the overlapping of different breast structures in the path of the X-ray beam that could interfere with cancer detection. Indeed, it is a 2-D projection image from a 3-D breast volume. For this reason, deeply buried tumors could be obscured by normal tissue making difficult their detection. On the contrary, normal tissues can be hidden by an artifact, leading to a false-positive result [13], [14].

Several studies have been carried out to improve image quality in radiographic exams, by developing suitable denoising and feature detection techniques, aiming to reduce the dose absorption [15]–[20]. Moreover, to overcome the limitation of conventional mammography, a lot of 3-D breast imaging techniques have been developed [8], [21]; among them breast tomosynthesis (BT) appears as one of the most promising techniques.

Digital BT allows reconstructing volumetric breast images from a finite number of low dose 2-D projections. These 2-D images are obtained by moving the X-ray tube along an arc around the breast with an angular range which typically does not exceed 60° .This technique improves the lesion visibility and allows an early breast cancer recognition, especially in women with radiographically dense breasts.

Although BT offers promising benefit, its use in breast cancer screening is under investigation because the quality of tomographic images is directly related to the radiation dose on the patient and it is significantly affected by the configuration parameters set by the technician during the mammographic exam. Normally, BT provides an increase in radiation dose with respect to 2-D mammography that sometimes is approximately and improperly indicted as double [22]. Then, it is

Manuscript received September 02, 2016; revised March 09, 2017; accepted March 15, 2017. Date of publication April 24, 2017; date of current version September 13, 2017. The Associate Editor coordinating the review process was Dr. Amitava Chatterjee. *(Corresponding author: Anna M. L. Lanzolla.)*

G. Andria, F. Attivissimo, A. Di Nisio, A. M. L. Lanzolla, and M. Spadavecchia are with the Department of Electrical and Information Engineering, Politecnico di Bari, 70125 Bari, Italy (e-mail: anna.lanzolla@poliba.it).

A. Maiorana and M. Mangiatini are with the Department of Med- ical Physics, Scientific Institute Hospital "Casa Sollievo della Sofferenza," 71013 San Giovanni Rotondo, Italy (e-mail: a.maiorana@operapadrepio.it; m.mangiantini@operapadrepio.it).

© 2017 IEEE. 2017 IEEE. Personal use is permitted. Permission from IEEE must be obtained for all other use, in any current or future media, including reprinting/republishing this material for advertising or promotional purpose, creating new collective works, for resale or redistribution to serves or list, or reuse of any copyright for this work in other works.

Fig. 1. Senographe essential by General Electric.

important to investigate the relationship between dose increasing and the effective improvement of image quality.

More recently, several studies have investigated the radiation risk in digital BT, but a limited number of works have compared the absorbed dose in BT and traditional mammography and quantified risks and benefits. Some studies assert that tomosynthesis offers superior performance in terms of lesion visibility with respect to traditional mammography basing only on subjective image evaluation by radiologist and the estimation of cancer detection rate and false-positive rate [3], [22]. In other works, the increase in dose is quantified but the corresponding improvement in terms of image quality is measured only by means of subjective evaluation [23].

The aim of this paper was to compare quantitatively the performances of tomosynthesis versus 2-D digital mammography by using both a well-accepted method to calculate the radiation dose and a suitable phantom for objective assessing of quality image in terms of contrast-to-noise ratio (*CNR*) rather than subjective evaluation. In Section II, the radiation dose to the patient is compared for both modalities, tomosynthesis and 2-D, confirming a general dose increase for tomosynthesis. In Section III, image quality and dose are evaluated by performing the test on reference targets in order to evaluate the tradeoff between increased image quality and increased dose of tomosynthesis.

II. Dosimetric Characterization

To characterize the dosimetric properties of BT it is necessary to evaluate the relationship between the image quality and the radiation dose absorbed by the patients during mammographic exams. The *average glandular dose* (AGD) [25] is the dosimetric quantity normally used to estimate the radiation dose and to evaluate the quality of the mammographic systems.

It represents the average absorbed dose in the glandular tissue in a uniformly compressed breast and depends on X-ray beam quality, breast thickness, and tissues composition. Due to the difficulty to directly evaluate the AGD, suitable relationships were used basing on the measurement of Entrance Surface Air Kerma [25], multiplied by appropriate conversion factors which consider the X-ray absorption dependence on: breast thickness, its composition and characteristics of the X-ray beam used.

Different techniques were proposed to evaluate the AGD, which are typically based on Monte Carlo method [26]–[29]. The most used relation for digital mammography can be found in [28] and [29]

$$\mathrm{AGD}_{2\text{-D}} = K \cdot g \cdot c \cdot s \tag{1}$$

where K is the Entrance Surface Air Kerma, without backscattering, which is expressed in milligray (mGy) and represents the amount of energy incident on the top surface of breast. The other parameters are conversion factors:

1) g, gives the AGD for a breast of glandularity 50% and is tabulated against *half value layer* (HVL) and breast thickness (see [25, Tables A5.1 and A5.5] for breast simulated with phantom and real case, respectively);
2) c, allows for breasts of different glandularity and is tabulated against HVL and breast thickness for typical breast compositions (see [25, Table A5.2] for breast simulated with phantom and [25, Tables A5.6 and A5.7] for real case with the age range 50 to 64 and 40 to 49, respectively);
3) s, takes into account the use of different X-ray spectra and depends on target/filter choice (see [25, Table A5.3]).

HVL represents the thickness of absorber which attenuates the air kerma of nonmonochromatic X-ray beams by half, therefore it characterizes the penetration capability of X-ray beams. The absorber normally used to evaluate HVL of low- energy X-ray beams, such as the ones used for mammography, is high-purity aluminum, thus HVL is commonly expressed as millimeters of aluminum.

In BT, the AGD is the sum of the doses received from individual projections and is evaluated in the following way [30]:

$$\mathrm{AGD}_{\mathrm{tomo}} = K \cdot g \cdot c \cdot s \cdot T \tag{2}$$

where T takes in account the range of projection angles. It is tabulated against breast thickness and projection angle (see [30, Tables A2.10 and A2.11] for breast simulated with phan- tom and real case, respectively). Equations (1) and (2) permit the AGD calculation when the Entrance Surface Air Kerma is known. According to the parametrical approach proposed in [31], it is possible to evaluate K for any value of the tube voltage in the range 25–32 kV, starting on measurements carried out at a specific distance from X-ray tube focus, at a tube voltage of 28 kV and for different target/filter combinations, by using the following equation:

$$t_{\mathrm{out}} = \frac{K}{t_l} = A \cdot V_t^{\,n} \tag{3}$$

where t_l is the tube current-exposure time product, called *tube loading*, V_t is the tube voltage, n is a constant which is tabulated against the target/filter combinations ([31, Table I]), and A is a constant which should be experimentally estimated. The ratio between air kerma and tube loading t_{out} is also called *X-ray tube output*.

TABLE I
SENOGRAPHE ESSENTIAL SPECIFICATIONS

Tube voltage range	*22 – 49 kV*
Tube loading range	*4 – 500 mAs*
Target	*Mo/Rh*
Filter	*Mo: 30 μm ; Rh: 25 μm*
Detector material	*CsI-Si*
Detector size	*24 x 31 cm²*
Angular Range	*± 12,5°*
Number of projections	*9*

It is necessary to evaluate the HVL because the conversion factors c and g in (1) and (2) depend on it. By using the parametric method of Robson [31], the HVL can be expressed as a quadratic function of tube voltage

$$\mathrm{HVL} = a \cdot V_t^2 + b \cdot V_t + c_H \tag{4}$$

where $a$and b are coefficients tabulated against the target/filter combinations ([31, Table I]) and c_H is a constant which has to be estimated experimentally.

A. Characterization of the Used Tomosynthesis System

Different experiments were carried out with the Research Hospital "Casa Sollievo della Sofferenza" (San Giovanni Rotondo, Italy) to characterize the BT equipment under test, which is a "Senographe Essential" by General Electric Healthcare shown in Fig. 1 [32]. This system provides both 2-D traditional mammography and 3-D tomosynthesis images. Its main technical specifications are listed in Table I. It is equipped with *automatic exposure control* (AEC) [33], a specific operation mode by which the tube loading is automatically controlled so that a specified radiation exposure is reached on a dose detector located under the image receptor. The *AEC* allows also the automatic selection of tube loading, target and filter combination.

In a first step, the coefficient A of (3) was empirically evaluated according to the procedure described in [31]. To this end, the calibrated dosimeter Piranha by RTI [34] was used. It permits to measure different quantities, such as tube voltage, exposition time, and radiation dose with the accuracy specifications listed in Table II.

The procedure for A calculation requires the measurement of K with the tube voltage set to a nominal value of 28 kV. To assess the reliability of tube voltage values provided by the tomosynthesis system, repeated measurements of tube voltage were performed for different target/filter combinations. The results, listed in Table III, show a deviation of measurement values V_{tm} with respect to the nominal value E_{vt}, always less than 0.5 kV, according to the "European guidelines for quality assurance in breast cancer screening and diagnosis" [25] which requires a reproducibility of ± 0.5 kV. Additional tests were carried out by varying the tube voltage in the range 25–32 kV and obtaining a maximum deviation of 0.35 kV.

Then, A was calculated by measuring K for different target/filter combinations and by applying (3), as shown in Table IV.

To measure K , the compression paddle of the tomosynthesis system is placed in the beam far away from the dose meter, so that the scatter contribution of the measurement device is reduced. Moreover, a constant Forwad Scatter Factor, $FSF = 1.076$, is used to correct the measured values [35].

Successively, the coefficient c_H in (4) was calculated. To this end, it is necessary to evaluate HVL by means of the following relationship [25]

$$\mathrm{HVL} = \frac{th_2 \cdot \ln\left(\frac{2 \cdot K_1}{K_0}\right) - th_1 \cdot \ln\left(\frac{2 \cdot K_2}{K_0}\right)}{\ln\left(\frac{K_1}{K_2}\right)} \tag{5}$$

where $K_o$is the incident air kerma measured with the Piranha device, with V_t 28 kV, while K_1 and $K_2$are air kerma measured by adding aluminum plates of thickness $th_1 = 0.1$ mm and th_2 0.2 mm, respectively. Table V shows the obtained coefficients c_H for different targets/filters.

Once the three coefficients of (4) are known, it is possible to evaluate HVL for any tube voltages as shown in Fig. 2. It is possible to note that the Rh/Rh combination provides highest HVL values, hence the use of rhodium for both target and filter results in X-ray penetration higher than other combinations. Consequently, for this device, it is advisable to use the Rh/Rh combination when high-thickness breast have to be examined.

B. Evaluation of Radiation Dose in Real Case

The reliability of the previously described coefficients calculation method was verified on a sample made by 100 patients who had undergone mammographic exams for cancer screening, performed in Research Hospital "Casa del Sollievo della Sofferenza"–San Giovanni Rotondo, Italy by using the characterized Senographe Essential system. The sample consists of 8% of patients under 40 years, 56% with age ranging in 40–50 years, and 36% over 50 years.

Each patient was carried out the mammographic exam in both 2-D and 3-D modality, according to the diagnostic protocol recommended by European guidelines [30] and for each of them, technical data and dose estimation values have been stored in a dedicated Hospital database. The acquired data were postprocessed, and results were analyzed to compare the performance of BT with respect to traditional mammog- raphy. Fig. 3 shows two mammographic images acquired by the same patient, with 2-D and tomosynthesis modality, respectively.

The parameters set by *AEC* are listed in Tables VI and VII. Tables VI and VII show that as the breast thickness increases, both tube loading and tube voltage have to rise in order to obtain high signal level and high tissue penetration, respectively. Moreover, for higher breast thickness, the best target/filter combination is Rh/Rh, otherwise it is preferable to use Mo/Rh or Mo/Mo (only for 2-D modality). This agrees with the results obtained for the system characterization previously performed.

TABLE II
PIRANHA RTI SPECIFICATIONS

Target/filter combinations		Mo/Mo, Mo/Rh, Mo/Al, Rh/Rh, W/Al, W/Rh, W/Ag	
Quantity		Range	Accuracy
Tube Voltage	Mo/Mo	18 – 49 kV	±1.5 % or ±0.7 kV
	Mo/Rh	22 – 46 kV	±2 % or ±1 kV
	Rh/Rh	25 – 49 kV	±2 % or ±1 kV
Exposition time		0.1 ms – 2000 s	±1 % or ±0.5 ms
Radiation dose		25 nGy – 1500 Gy	± 5 %
Radiation dose rate		25 nGy/s – 750 mGy/s	± 5 %

TABLE III
REPEATED MEASUREMENTS OF TUBE VOLTAGE FOR DIFFERENT TARGETS/FILTERS

	Mo/Mo		Mo/Rh		Rh/Rh	
V_{tn} [kVp]	V_{tm} [kVp]	E_{vt}[kVp]	V_{tm} [kV]	E_{vt} [kVp]	V_{tm} [kV]	E_{vt} [kVp]
28	27.55	-0.45	27.58	-0.42	27.56	-0.44
28	27.56	-0.44	27.57	-0.43	27.54	-0.46
28	27.58	-0.42	27.55	-0.45	27.59	-0.41
28	27.56	-0.44	27.62	-0.38	27.63	-0.37
28	27.62	-0.38	27.55	-0.45	27.61	-0.39
28	27.57	-0.43	27.53	-0.47	27.61	-0.39
28	27.64	-0.36	27.61	-0.39	27.55	-0.45
28	27.56	-0.44	27.6	-0.4	27.57	-0.43
28	27.59	-0.41	27.56	-0.44	27.64	-0.36
28	27.63	-0.37	27.59	-0.41	27.58	-0.42

TABLE IV
CALCULATION OF A FOR DIFFERENT TARGETS/FILTERS

Target/filter	V_t [kVp]	t_l [mAs]	K [mGy]	t_{out} [mGy/mAs]	n	A
Mo/Mo	28	50	4.954	0.09908	3.06	$\mathbf{3.87 \times 10^{-6}}$
Mo/Rh	28	50	4.107	0.08214	3.24	$\mathbf{1.77 \times 10^{-6}}$
Rh/Rh	28	50	3.791	0.07582	3.03	$\mathbf{3.27 \times 10^{-6}}$

Successively, the values of the radiation dose obtained in 2-D and 3-D acquisition were analyzed.

Fig. 4 shows the values of AGD provided by the tomographic system obtained in both 2-D and tomosynthesis acquisitions as a function of breast thickness; the red line represents the acceptable boundary limit stated in European Protocol for digital mammography [36].

It is possible to note that for thickness values less than 55 mm the glandular dose is similar for both modali- ties; instead, for higher breast thickness the tomosynthesis provides a dose level greater than 2-D acquisition. This depends on the configuration parameters of the AEC system. Tables VI and VII show that in the thickness range 60–70 mm, for the same selection of target/filter and tube voltage, the tomosynthesis provides tube loading greater than 2-D acquisition hence higher radiation dose.

Finally, the AGD was calculated by using (1) and (2).

It has to be considered that the air kerma previously calculated by means of the parametric method is referred to a fixed distance between focal spot and breast support (d_{fb} = 660 mm for the tested system). In the real case, the X-ray attenuation due to breast thickness has to be considered. Then,

TABLE V
C_H VALUE FOR DIFFERENT TARGETS/FILTERS

	Mo/Mo	**Mo/Rh**	**Mo/Rh**
V_t **[kVp]**	28	28	28
t_l **[mAs]**	50	50	50
K_0 **[mGy]**	4.804	3.991	3.686
K_1 **[mGy]**	3.964	3.348	3.106
K_2 **[mGy]**	3.308	2.841	2.645
a	-0.000326	-0.000624	-0.000514
b	0.0273	0.0445	0.0425
c_H	**-0.13190906**	**-0.34165228**	**-0.36216037**

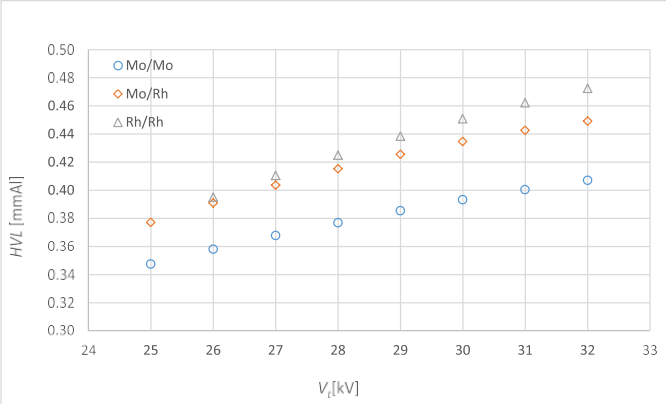

Fig. 2. HVL versus V_t for different target/filter combinations.

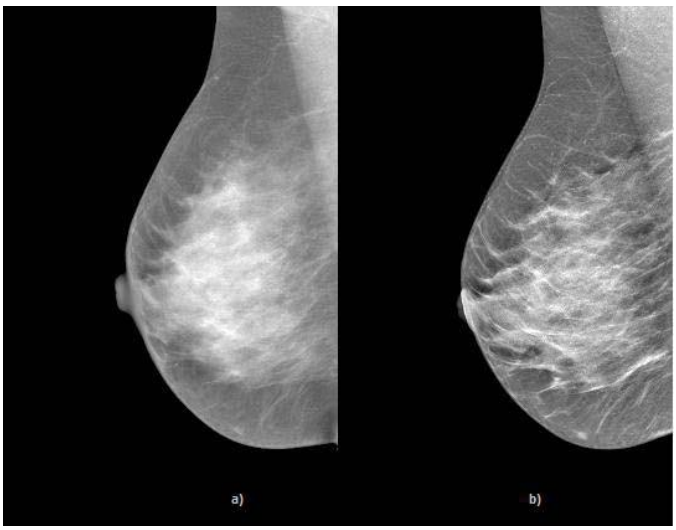

Fig. 3. Mammograpic images acquired with (a) 2-D and (b) tomosyntes modality. The latter appears to have more contrast and details.

considering the inverse square dependence of air kerma on distance, the following relationship has to be used:

$$K_r = K \cdot \frac{(d_{fb} - \text{th}_m)^2}{[d_{fb} - (\text{th}_b - \text{th}_m)]^2} \quad (6)$$

where K_r is the air kerma evaluated for the real case, th_m = 7.5 mm is the dosimeter thickness, and th_b is the compressed breast thickness provided by the tomographic system, measured as distance between X-ray receptor and compression paddle.

Fig. 5 compares AGD values provided by the tested system in the tomographic modality with values obtained by combining (2) and (6) and shows a good agreement of the results, with a 0.96 correlation coefficient obtained by applying the least mean square method. However, the tomographic system systematically underestimates the radiation dose by 15% on average as also shown in previous study obtained by using the same dose calculation method and same dosimeter [23]. This could be due to the variation of dosimetric characteri- zation coefficients with time and this is the reason why the European Guidelines recommend to execute calibration tests periodically (every six months). Moreover, the method used by the manufacturer to estimate the AGD is actually unknown.

III. IMAGE QUALITY EVALUATION

The characteristics of the radiation beams provided by mammographic devices depend on different configuration parameters, such as target/filter combination, tube voltage, and tube loading [37]. The setting of these parameters affects the shape and the intensity of the signal spectrum and the level of penetration of the X-ray beam.

In the proposed study, the performance of the tomographic system under test, in terms of image quality, was evalu- ated using a TOR MAX phantom (Fig. 6) by Leed Test Objects [38], which has a uniform background and includes different physical object details; it permits to carry out the following tests:

1) *sensitometry* (Ten-step grey-scale plus two points for Sensitometric measurements);
2) *high-Resolution limit* (1 to 20 LP/mm);
3) *low Contrast Resolution* (1.8 to 5 line pairs/mm, repre- senting filamentary structures);
4) *low-contrast large-detail detectability* (12 details, 5.6- mm diameter with manufacturing tolerance of 5%);
5) *high-contrast small-detail detectability* (11 details, 0.5- and 0.25-mm diameter with manufacturing toler- ance of ±5%).

The phantom consists of eight polymethyl methacry- late (PMMA) slabs with thickness ranging from 10 to 60 mm (see Fig. 7) and is used to emulate the attenuation of variously sized breasts in order to assess the incident radiation dose.

To evaluate the performance of the radiological equipment under test, TOR MAX images were analyzed with Automatic Phantom Image Analysis software by Cyberqual [39], which automatically recognizes the details associated with the X-ray image and quickly calculates quality image indexes.

Image quality can objectively be estimated using several metrics defined in the literature, such as image noise, contrast, and spatial resolution, and depends on several factors including

TABLE VI
PARAMETERS FOR 2-D ACQUISITION

	Mo/Mo			Mo/Rh			Rh/Rh		
	Tube voltage (kV)			Tube voltage (kV)			Tube voltage (kV)		
	26	27	28	27	28	29	29	30	31
breast thickness [mm]	t_l (mAs)	t_l (mAs)	t_l (mAs)	t_l (mAs)	t_l (mAs)	t_l (mAs)	t_l (mAs)	t_l (mAs)	t_l (mAs)
20 - 30	45 - 50	-	50 - 60	-	-	-	-	-	-
30 - 40	50 -60	60 – 70	50 - 60	40 – 60	50 - 70	-	-	-	-
40 - 50	-	-	60 - 70	50 – 70	60 - 80	-	45 - 70	-	-
50 - 60	-	-	-	-	-	100 - 110	50 - 80	60 - 75	60 - 70
60 - 70	-	-	-	-	-	-	65 - 90	70 - 80	65 - 75

TABLE VII
PARAMETERS FOR TOMOSYNTHESIS ACQUISITION

	Mo/Rh		Rh/Rh	
	Tube voltage (kV)		Tube voltage (kV)	
	26	27	29	31
breast thickness [mm]	t_l (mA)	t_l (mA)	t_l (mA)	t_l (mA)
20 - 30	45 - 55	45 – 60	-	-
30 - 40	-	-	35 – 55	-
50	-	-	45 – 70	-
60	-	-	55 – 75	-
70	-	-	65 – 90	70 - 100

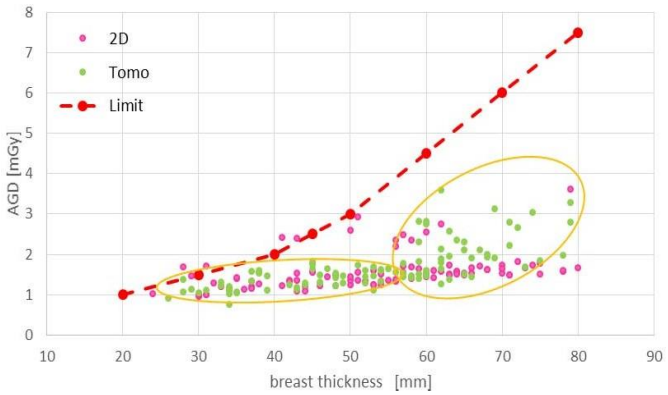

Fig. 4. AGD versus breast thickness.

sensors accuracy, signal quality, and performance of analog-to-digital converters [40]–[44].

In the experiments, *CNR* was used because its capability in quantifying the visibility of details in a noisy image

making it the most used index in assessing of breast image quality [46]–[49]

$$\mathrm{CNR} = \frac{|\mu_d - \mu_b|}{\sigma_b} \tag{7}$$

where μ_d and μ_b are the mean pixel value of detail and of background, respectively, and σ_b is the standard deviation of pixel values of background. The detail is individuated as a circular area well inside the border of high-intensity pixels. Achieving a high separation between μ_d and μ_b with a small σ_b is important also when techniques for automatic detection of lesions are considered. Indeed, in this case, the choice of detection thresholds, one of the most critical tasks in medical as well as industrial image processing [50], [51], is greatly simplified.

A second metric, *details counts contrast* (*DCC*), was also used to further quantify breast image quality. It is defined as

$$\mathrm{DCC} = \frac{1}{\#D} \sum_{i \in D} \frac{|I_i - \mu_b|}{\sigma_b} \tag{8}$$

where: I_i is the value of pixel i of image I ; D is the set of pixels belonging to the detail, defined as those pixels having value greater than $\mu_b + \sigma_b$; and $\#D$ is the number of pixels of the detail. While *CNR* is computed for pixels inside a circle, *DCC* is computed for pixels selected according to their difference with respect to background and includes pixels near the border of the detail. In general, the difference between

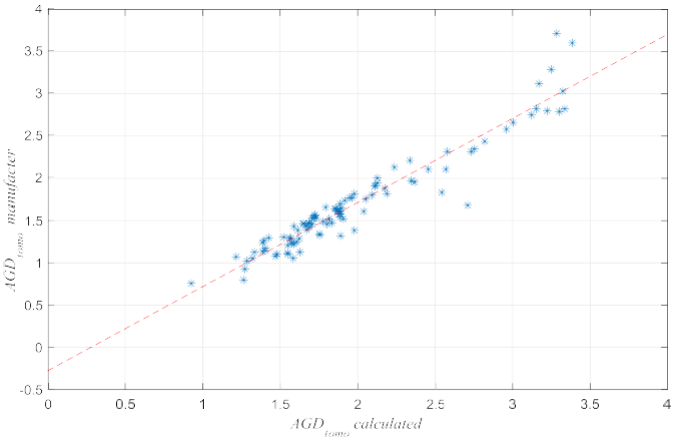

Fig. 5. AGD provided by the tested system in the tomographic modality versus the calculated AGD and (dashed) linear regression.

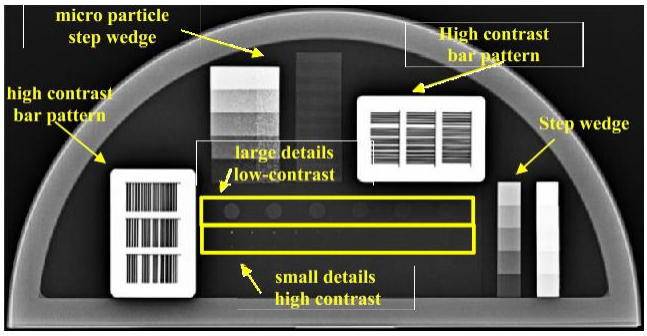

Fig. 6. TOR MAX X-ray image.

Fig. 7. Slabs of PMMA simulating the breast model.

CNR and *DCC* can be appreciated for small details. Different image quality tests were performed by varying the thickness of PMMA slabs; for each test, the AGD was calculated as previously described. It should be noted that PMMA is denser than breast tissue, and then a suitable conversion from PMMA thickness to equivalent breast thickness was proposed in [25] and reported in Table VIII. These equivalent thicknesses have to be used in (6) for a correct air kerma calculation.

In this paper, attention has been paid to small details recognition, because of the great importance of small lesion

TABLE VIII
CONVERSION FROM PMMA THICKNESS TO BREAST THICKNESS [25]

PMMA thickness [mm]	Equivalent breast thickness[mm]
20	21
30	32
40	45
45	53
50	60
60	75
70	90
80	103

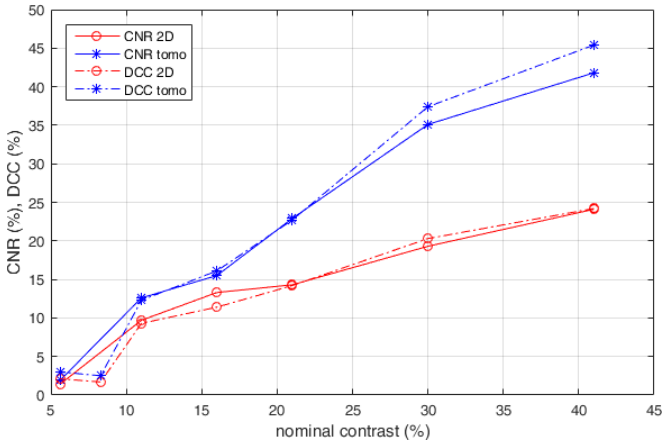

Fig. 8. CNR and DCC versus nominal contrast for small details (0.5-mm diameter) for 2-D and tomosynthesis acquisitions, with 40 mm of PMMA thickness. *AG D* is 1.27 mGy for CNR and 1.46 mGy for tomosynthesis.

detection for breast cancer screening. For the TOR MAX phantom these small details consist of circular areas with 0.5-mm diameter and with nominal contrast (defined as the signal difference of a detail with respect to the background) decreasing from 41% to 1.5%.

Fig. 8 shows the behavior of *CNR* as a function of nom- inal contrast for 0.5-mm-small details, for both 2-D and BT modality test, by using a 40-mm combination of PMMA slabs representing the standard breast thickness of 45 mm. It is possible to observe that even if BT provides an increase in glandular dose of 15% with respect to 2-D acquisition, it offers best performance with about 62% average *CNR* increase. This improvement is particularly evident in high levels of nominal contrast. It is confirmed also by the behavior of the *DCC*, which is uniformly higher for tomosynthesis. The same tests were carried out for small details with 0.25-mm diameter, obtaining similar results. In this case, BT provides a CNR average increase of 46%, while the increase in glandular dose is the same (15%) because the acquisition parameters influ- encing the AGD calculation (tube voltage, tube loading, and target/filter combination) depend only on PMMA (or breast) thickness.

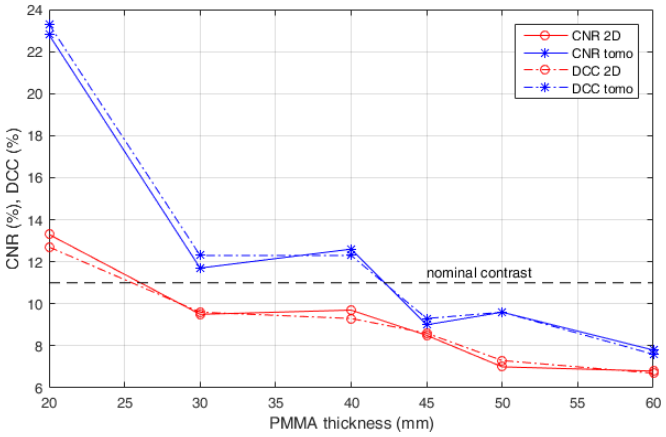

Fig. 9. CNR and DCC versus PMMA thickness for detail of 0.5-mm diameter and 11% nominal contrast (black line).

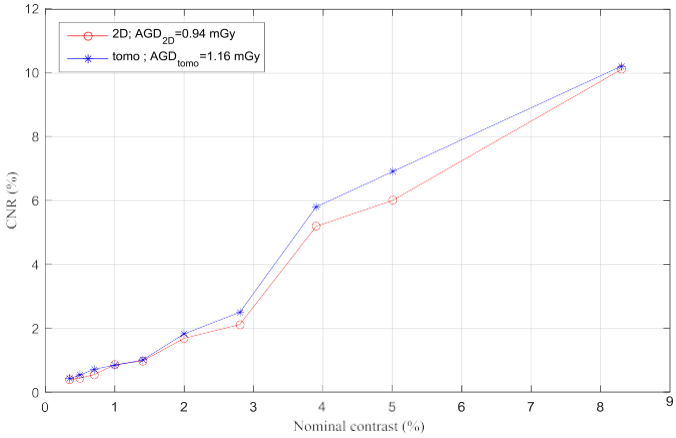

Fig. 11. CNR values versus nominal contrast for large details (5.6-mm diameter) for 2-D and tomosynthesis acquisitions.

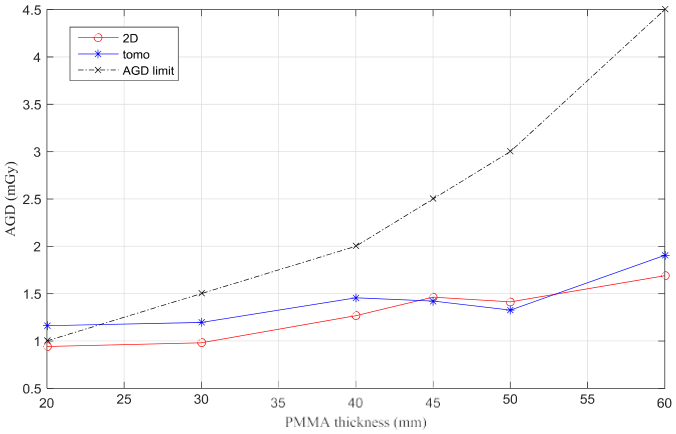

Fig. 10. AGD values versus PMMA thickness; the black line represents AGD limit values.

Therefore, the behavior of *CNR* and*DCC* as a function of slabs thickness was analyzed for a fixed detail. In particular, the detail with nominal contrast of 11% was considered, representing the worst experimental condition. The results confirm the best performance of BT with an average *CNR* increase of about 31% with respect to 2-D, while the AGD increases of 15% on average. The *CNR* behavior is similar for both acquisition modalities and decreases as the PMMA thickness increases (as shown in Fig. 9). For low-PMMA thickness values, tomosynthesis provides *CNR* and *DCC* values higher than the nominal contrast.

Fig. 10 compares AGD versus PMMA thickness for 2-D and tomosynthesis acquisition. It can be noted that tomosyn- thesis provides a higher radiation dose (maximum 23%) but the difference decreases as the PMMA thickness increases. Moreover, for PMMA thickness in the range 45–50 mm, AGD values in tomosynthesis are lower than in 2-D acquisition. It should be also noted that any automatic selection of tube voltage, tube loading, and target/filter may be slightly different for real breasts since, as already said, PMMA is denser than breast tissue.

The obtained AGD values are always below the limits stated in [36], except for tomosynthesis modality for 20 mmof PMMA thickness where the glandular dose slightly overcomes the recommended limit. As shown in Fig. 9, for low PMMA thickness, tomosynthesis provides *CNR* values much higher than the nominal contrast, and thus, it is advisable to modify *AEC* settings to reduce the glandular dose (for example, by decreasing the tube loading) without prejudice to image quality.

Finally, the system performance for low-contrast large-details (diameter of 5.6 mm) was investigated. Fig. 11 shows that tomosynthesis offers best results, in terms of *CNR* val- ues (average increase of 12%), with respect to 2-D modality.

IV. Conclusion

In this paper, the advantage of using tomosynthesis technology for breast cancer detection was analyzed and the best choice of configuration parameters was explored. To evaluate the performance of BT in terms of both radiation dose and image quality, several experimental tests were carried out comparing the results obtained with a tomographic device able to carry out mammographic exams in both 2-D and tomosynthesis modality.

This paper shows that the use of tomosynthesis techniques is particularly suitable for detecting small details in moderate contrast images. Indeed, even if the tomosynthesis provides an increase of about 15% in AGD with respect to 2-D modality, it offers improvement higher than 30% in *CNR* for small details with high contrast. For large details with low contrast, BT offers an average *CNR* increase of 12%.

Moreover, the experimental results have pointed out a tendency of mammographic system to provide an under estimate of the mean glandular dose.

Acknowledgment

The authors would like to thank the clinical staff of Research Hospital “Casa del Sollievo della Sofferenza”—San Giovanni Rotondo, Italy—for providing data and valuable information used for the proposed study and for their helpful discussions.

REFERENCES

[1] H. Weedon-Fekjær, P. R. Romundstad, and L. J. Vatten, "Modern mammography screening and breast cancer mortality: Population study," *Brit. Med. J.*, vol. 348, p. g3701, Jul. 2014.

[2] R. E. Hendrick and M. A. Helvie, "Mammography screening: A new estimate of number needed to screen to prevent one breast cancer death," *Amer. J. Roentenol.*, vol. 198, no. 3, pp. 723–728, Mar. 2012.

[3] S. P. Poplack, T. D. Tosteson, C. A. Kogel, and H. M. Nagy, "Digital breast tomosynthesis: initial experience in 98 women with abnormal digital screening mammography," *Amer. J. Roentenol.*, vol. 189, no. 3, pp. 616–623, Sep. 2007.

[4] G. Gennaro *et al.*, "Digital breast tomosynthesis versus digital mammography: A clinical performance study," *Eur. Radiol.*, vol. 20, no. 7, pp. 1545–1553, Jul. 2010.

[5] F. Attivissimo, G. Cavone, A. M. L. Lanzolla, and M. Spadavecchia, "A technique to improve the image quality in computer tomography," *IEEE Trans. Instrum. Meas.*, vol. 59, no. 5, pp. 1251–1257, May 2010.

[6] C. J. Martin, P. F. Sharp, and D. G. Sutton, "Measurement of image quality in diagnostic radiology," *Appl. Radiat. Isotopes*, vol. 50, pp. 21–38, Jan. 1999.

[7] C. M. Sehgal, S. P. Weinstein, P. H. Arger, and E. F. Conant, "A review of breast ultrasound," *J. Mammary Gland Biol. Neoplasia*, vol. 11, no. 2, pp. 113–123, Apr. 2006.

[8] E. Yin-Kwee, E. Y.-K. Ng, R. U. Acharya, and O. Faust, "Breast imaging: A survey," *World J. Clin. Oncol.*, vol. 2, no. 4, pp. 171–178, Apr. 2011.

[9] E. Porter, A. Santorelli, and M. Popovic, "Time-domain microwave radar applied to breast imaging: Measurement reliability in a clini- cal setting," *Prog. Electromagn. Res.*, vol. 149, pp. 119–132, 2014, doi: 10.2528/PIER14080503.

[10] G. Quarto *et al.*, "Estimate of tissue composition in malignant and benign breast lesions by time-domain optical mammography," *Biomed. Opt. Exp.*, vol. 5, no. 10, pp. 3684–3698, Oct. 2014.

[11] A. Cataldo, L. Tarricone, F. Attivissimo, and A. Trotta, "Simultaneous measurement of dielectric properties and levels of liquids using a TDR method," *Measurement*, vol. 41, no. 3, pp. 307–319, Apr. 2008.

[12] A. Cataldo, L. Catarinucci, L. Tarricone, F. Attivissimo, and E. Piuzzi, "A combined TD–FD method for enhanced reflectometry measurements in liquid quality monitoring," *IEEE Trans. Instrum. Meas.*, vol. 58, no. 10, pp. 3534–3543, Oct. 2009.

[13] M. B. Williams *et al.*, "Digital radiography image quality: Image acquisition," *J. Amer. College Radiol.*, vol. 4, no. 6, pp. 371–388, Jun. 2007.

[14] G. Andria, F. Attivissimo, A. M. L. Lanzolla, and M. Savino, "A suitable threshold for speckle reduction in ultrasound images," *IEEE Trans. Instrum. Meas.*, vol. 62, no. 8, pp. 2270–2279, Aug. 2013.

[15] A. Mencattini, M. Salmeri, R. Lojacono, M. Frigerio, and F. Caselli, "Mammographic images enhancement and denoising for breast cancer detection using dyadic wavelet processing," *IEEE Trans. Instrum. Meas.*, vol. 57, no. 7, pp. 1422–1430, Jul. 2008.

[16] G. Andria, F. Attivissimo, A. di Nisio, A. M. L. Lanzolla, G. Guglielmi, and R. Terlizzi, "Dose optimization in chest radiography: System and model characterization via experimental investigation," *IEEE Trans. Instrum. Meas.*, vol. 63, no. 5, pp. 1163–1170, May 2014.

[17] K. Hu, X. Gao, and F. Li, "Detection of suspicious lesions by adaptive thresholding based on multiresolution analysis in mammograms," *IEEE Trans. Instrum. Meas.*, vol. 60, no. 2, pp. 462–472, Feb. 2011.

[18] G. Andria, F. Attivissimo, G. Guglielmi, A. M. L. Lanzolla, A. Maiorana, and M. Mangiantini, "Towards patient dose optimization in digital radiography," *Measurement*, vol. 79, pp. 331–338, Feb. 2016.

[19] N. Szekely, N. Toth, and B. Pataki, "A hybrid system for detecting masses in mammographic images," *IEEE Trans. Instrum. Meas.*, vol. 55, no. 3, pp. 944–952, Jun. 2006.

[20] A. Mencattini, G. Rabottino, S. Salicone, and M. Salmeri, "Uncertainty modeling and propagation through RFVs for the assessment of CADx systems in digital mammography," *IEEE Trans. Instrum. Meas.*, vol. 59, no. 1, pp. 27–38, Jan. 2010.

[21] L. Kovacs *et al.*, "Original article Comparison between breast vol- ume measurement using 3D surface imaging and classical techniques," *Breast*, vol. 16, no. 2, pp. 137–145, Apr. 2007.

[22] P. Skaane *et al.*, "Comparison of digital mammography alone and digital mammography plus tomosynthesis in a population-based screening program," *Radiology*, vol. 267, no. 1, pp. 47–56, Apr. 2013.

[23] E. Meybluma *et al.*, "Breast tomosynthesis: Dosimetry and image quality assessment on phantom," *Diagnostic Interventional Imag.*, vol. 96, no. 9, pp. 931–939, Sep. 2015.

[24] A. Samani, J. Bishop, M. J. Yaffe, and D. B. Plewes, "Biomechanical 3-D finite element modeling of the human breast using MRI data," *IEEE Trans. Med. Imag.*, vol. 20, no. 4, pp. 271–279, Apr. 2001.

[25] N. Perry, M. Broeders, C. de Wolf, S. Törnberg, R. Holland, and L. von Karsa, "European guidelines for quality assurance in breast cancer screening and diagnosis," in *Health Consumer Protection Directorate-General*, 2006.

[26] X. Wu, T. Barnes, and D. M. Tucker, "Spectral dependence of glan- dular tissue dose in screen-film mammography," *Radiology*, vol. 179, pp. 143–148, Apr. 1991.

[27] X. Wu, T. Barnes, E. L. D. Gingold, and M. Tucker, "Normalized average glandular dose in molybdenum target-rhodium filter and rhodium target-rhodium filter mammography," *Radiology*, vol. 89, pp. 83–89, Oct. 1994.

[28] D. R. Dance, C. L. Skinner, K. C. Young, J. R. Beckett, and C. J. Kotre, "Additional factors for the estimation of mean glandular breast dose using the UK mammography dosimetry protocol," *Phys. Med. Biol.*, vol. 45, no. 11, pp. 3225–3240, Nov. 2000.

[29] D. R. Dance, K. C. Young, and J. R. Beckett, "Further factors for the estimation of mean glandular dose using the United Kingdom, European and IAEA breast dosimetry protocols," *Phys. Med. Biol.*, vol. 54, pp. 4361–4372, Jul. 2009.

[30] A. Burch *et al.*, "Routine quality control tests for breast tomosynthesis (physicists)," Public Health England, London, U.K., Tech. Rep. 1407, Dec. 2015

[31] K. J. Robson, "A parametric method for determining mammographic X-ray," *Brit. J. Radiol.*, vol. 74, no. 880, pp. 335–340, Apr. 2001.

[32] *Senographe Essential*, accessed on Mar. 2016. [Online]. Available: http://www3.gehealthcare.com/en/products/categories/mammography/senographe_essential/

[33] M. Söderberg and M. Gunnarsson, "Automatic exposure control in computed tomography–an evaluation of systems from different manufacturers," *Acta Radiol.*, vol. 51, no. 6, pp. 625–634, Jul. 2010.

[34] *Black Piranha*, accessed on Mar. 2016. [Online]. Available: http://rtigroup.com/products/product-detail/black-piranha

[35] P. Toroi, N. Könönen, M. Timonen, and M. Kortesniemi, "Aspects of forward scattering from compression paddle in the dosimetry of mammofraphy," *Radiation Protection Dosimetry*, vol. 154, no. 4, pp. 439–445, May 2013.

[36] R. E. van Engen *et al.*, "Protocol for the quality control of the physical and technical aspects of digital breast tomosynthesis systems," in *Proc. EUREF*, Nijmegen, The Netherlands, Jun. 2016.

[37] G. Andria, F. Attivissimo, A. di Nisio, A. M. L. Lanzolla, and M. Spadavecchia, "Image quality evaluation of breast tomosynthesis," in *Proc. MeMeA*, May 2016, pp. 143–148.

[38] *TOR MAX, Leeds Test Objects*, accessed on Mar. 2016. [Online]. Available: http://www.leedstestobjects.com/index.php/phantom/tor-max

[39] [Online]. Available: http://autopia.cyberqual.it/index.php/AutoPIA

[40] Z. Wang and A. C. Bovik, "A universal image quality index," *IEEE Signal Process. Lett.*, vol. 9, no. 3, pp. 81–84, Mar. 2002.

[41] G. Andria, F. Attivissimo, N. Giaquinto, A. M. L. Lanzolla, L. Quagliarella, and N. Sasanelli, "Functional evaluation of handgrip signals for parkinsonian patients," *IEEE Trans. Instrum. Meas.*, vol. 55, no. 5, pp. 1467–1473, Oct. 2006.

[42] G. C. Giakos *et al.*, "Detected contrast and dynamic range measurements of CdZnTe semiconductors for flat-panel digital radiography," *IEEE Trans. Instrum. Meas.*, vol. 50, no. 6, pp. 1604–1609, Dec. 2001.

[43] F. Attivissimo, N. Giaquinto, and M. Savino, "Worst-case uncertainty measurement in ADC-based instruments," *Comput. Standards Interfaces*, vol. 29, no. 1, pp. 5–10, Jan. 2007.

[44] A. Faro, D. Giordano, C. Spampinato, S. Ullo, and A. Di Stefano, "Basal ganglia activity measurement by automatic 3-D striatum segmentation in SPECT images," *IEEE Trans. Instrum. Meas.*, vol. 60, no. 10, pp. 3269–3280, Oct. 2011.

[45] F. Adamo, F. Attivissimo, and A. Di Nisio, "Calibration of an inspection system for online quality control of satin glass," *IEEE Trans. Instrum. Meas.*, vol. 59, no. 5, pp. 1035–1046, May 2010.

[46] M. M. Goodsitt *et al.*, "Digital breast tomosynthesis: Studies of the effects of acquisition geometry on contrast-to-noise ratio and observer preference of low-contrast objects in breast phantom images," *Phys. Med. Biol.*, vol. 59, no. 19, pp. 5883–5902, Oct. 2014.

[47] M. Baptista *et al.*, "Image quality and dose assessment in digital breast tomosynthesis: A Monte Carlo study," *Radiation Phys. Chem.*, vol. 104, pp. 158–162, Nov. 2014.

[48] X. Song *et al.*, "Automated region detection based on the contrast-to-noise ratio in near-infrared tomography," *Appl. Opt.*, vol. 43, no. 5, pp. 1053–1062, Feb. 2004.

[49] M. Skarpathiotakis *et al.*, "Development of contrast digital mammography," *Med. Phys.*, vol. 29, no. 10, pp. 2419–2426, Oct. 2002.
[50] F. Adamo, F. Attivissimo, A. di Nisio, and M. Spadavecchia, "An automatic document processing system for medical data extraction," *Measurement*, vol. 61, pp. 88–99, Feb. 2015.
[51] F. Adamo, F. Attivissimo, A. di Nisio, and M. Savino, "A low- cost inspection system for online defects assessment in satin glass," *Measurement*, vol. 42, no. 9, pp. 1304–1311, Nov. 2009.

Gregorio Andria (M'12) was born in Massafra, Italy, in 1956. He received the M.S. degree in electrical engineering and the Ph.D. degree in power systems from the State University of Bari, Bari, Italy, in 1981 and 1987, respectively.

He was with the Department of Electrical and Electronics, State University of Bari. He was involved in filtering design techniques to increase the performance of digital measuring instrumenta- tion. He is currently a Full Professor of Electrical Measurements with the Polytechnic of Bari, Bari, where he is involved in the optimization of spectral estimation algorithms for monitoring of distortion levels in power systems, robotics, and diagnostics of electrical drives. His current research interests include characterization of A/D converters, DSP techniques for time-frequency measurements on stochastic signals, and the characterization of intelligent instruments.

Filippo Attivissimo (M'11) received the M.S. and Ph.D. degrees in electronic engineering from the Polytechnic of Bari, Bari, Italy, in 1993 and 1997, respectively.

Since 1993, he has been with the Polytechnic of Bari, where he is involved in research projects in the field of digital signal processing for mea- surements, and is currently an Associate Professor of Electric and Electronic Measurements with the Electrical and Electronic Measurements Laboratory, Department of Electrical and Electronic Engineering. His current research interests include the electric and electronic measurement on devices and systems, estimation theory, uncertainty evaluation, design of sensors, medicine and transportation, digital measurements on power electronic systems, computer vision, and analog-to-digital converter modeling, characterization and optimization.

Dr. Attivissimo is a member of the Italian Association "Electrical and Electronic Measurements Group."

Attilio Di Nisio (M'14) was born in Bari, Italy, in 1980. He received the M.S. (Hons.) degree and the Ph.D. degree in electronic engineering from the Politecnico di Bari, Bari, Italy, in 2005 and 2009, respectively.

He is currently a Research Fellow with Politec- nico di Bari. His current research interests include DSP-based systems for power quality analysis, wire- less sensor networks, soil mechanics testing equip- ment, analog-to-digital and digital-to-analog con- verters modeling and testing, estimation theory, software for automatic test equipment, sensors, image processing for quality control applications and document understanding, medical imaging, and photovoltaic panels modeling and testing.

Dr. Nisio is a member of the IEEE I&M Society and the Italian Association of Electrical and Electronic Measurements Group.

Anna M. L. Lanzolla (M'11) received the M.S. degree in electronic engineering and the Ph.D. degree in electric engineering from the Polytechnic of Bari, Bari, Italy, in 1995 and 1999, respectively.

Since 1995, she has been with the Polytechnic of Bari, where she is involved in the field of digital signal processing for measurements and is currently an Assistant Professor with the Department of Electrics and Electronics. Her current research interests include electric and electronic measurement on devices and systems, including estimation theory, optimization of spectral estimation algorithms for monitoring of distortion levels in power systems, modeling techniques for monitoring and controlling of environmental quantities, image processing, and measurement for medical applications.

Dr. Lanzolla is a member of the Italian Group of Electrical and Electronic Measurements.

Alberto Maiorana received the M.S. degree in physics from the University of Rome "Sapienza," Rome, Italy, in 1984, and the Post-Graduate Diploma degree in medical physics from the University of Rome "Tor Vergata," Rome, in 1990.

Since 1986, he has been with the Medical Physics Department, IRCCS "Casa Sollievo della Sofferenza," San Giovanni Rotondo, Italy. His current research interests include radiotherapy and radiology physics, nuclear medicine physics, medical and environmental dosimetry, and image processing.

Dr. Maiorana is a member of the Italian Association of Medical Physics.

Marco Mangiantini received the M.S. degree in physics from the University of Rome "La Sapienza," Rome, Italy, in 1989, and the Post-Graduate Diploma degree in medical physics from the University of Rome "Tor Vergata," Rome, in 1998.

Since 1996, he has been with the Medical Physics Department, IRCCS "Casa Sollievo della Sofferenza," San Giovanni Rotondo, Italy. His current research interests include radiotherapy and radiology physics, nuclear medicine physics, medical and environmental dosimetry, and image processing.

Dr. Mangiantini is a member of the Italian Association of Medical Physics.

Maurizio Spadavecchia (S'11–M'14) received the M.S. (Hons.) and the Ph.D. degrees in electrical engineering from the Politecnico di Bari, Bari, Italy, in 2006 and 2011, respectively.

Since 2006, he has been with the Electrical and Electronic Measurements Laboratory, Politecnico di Bari, where he is currently a Research Fellow. His current research interests include electrics and electronics measurement on instruments and devices, the characterization of renewable energies devices, software for automatic test equipment, photovoltaic and thermoelectric modules modeling and testing, power quality systems and measurements, smart metering, and soil mechanics testing equipment.

Dr. Maurizio is a member of the IEEE Instrumentation and Measurements Society and the Italian association Electrical and Electronic Measurements Group.